Increasing chatter stability in robotic milling by kinematic redundancy

Bora Gonul[a], and Lutfi Taner Tunc[b]

a, Sabanci University, Faculty of Engineering and Natural Sciences, Integrated Manufacturing Research and Application Center,Istanbul/TURKEY,boragonul@sabanciuniv.edu
b, Sabanci University, Faculty of Engineering and Natural Sciences, Integrated Manufacturing Research and Application Center,Istanbul/TURKEY,ttunc@sabanciuniv.edu

Abstract

Robotic milling is exposed to significantly varying dynamic response at the tool tip due to varying serial kinematics and related dynamic properties of the robot. Therefore, conditions of stable cutting operation alter in working zone, where directional effect of the feed plays an important role. In this study, it has been investigated and demonstrated that the kinematic redundancy of 6-axis serial arm robots can be used to reach improved stable cutting conditions and the kinematic redundancy is used to eliminate the feed and position impacts on stability limits. The discussions are provided through simulations.

Keywords: Robotic Milling, Dynamics, Stability

1 Introduction

Industrial robots were intended to be utilized in monotonous works, for example, pick and place, material handling, painting, riveting and welding, where the necessary motion resistance is generally low and dynamic forces are not regenerative as milling. Companies' interest in low-cost and reconfigurable production infrastructures has played an important role in robotic manufacturing over the last decade. Industrial robots offer considerable supremacy that can be categorized as working envelope to footprint ratio, low capital investment and reprogrammability with respect to CNC machine tools. Conversely, industrial robots have certain disadvantages such as low tool path accuracy, less rigid structure due to serial articulated design leading to low-frequency chatter vibrations. Hereby, studies and investigations on dynamics and stability of robotic milling has attracted attention in the last decade [[2[6]. Chatter is one of the major constraints in milling, leading to low productivity and quality. Thus, it remained a topic of interest for more than 50 years [1]. Chatter issues in robotic milling was first researched by Oki and Kanitani [2] and Pan et al [3]. They showed that low-frequency modes in robotic milling are critical through mode coupling chatter, which is due to less stiff structure of the robot [3]. In robotic milling, alteration of the feed direction [4] or the robot configuration might be considered as alternative approach to accomplish expanded stability limits [5], where the latter provides a kind of gain from the kinematic redundancy. Bisu et al. [6] investigated the dynamic behavior of a 6-axis industrial robot for machining with a high-speed spindle attached. Their examination procedure comprises of three phases, targeting the self-excited chatter frequencies of the robot structure in various configurations while spindle is off and on without cutting. Then, they conducted the tests with cutting operation. At that point, they demonstrated the variety in the vibrations brought about by the robot structure, at various positions. Afterwards, Mejri et al. [5] evaluated the 6-axis industrial robot by experimental observation to calculate the stability lobes using the frequency domain solution in terms of milling stability with a high-speed spindle within the working area[7]. They investigated tool tip dynamics through positional dependancy of robot structure at various positions. The outcomes demonstrated that the process dynamics rely upon the robot position and the excitation course. In this way, feed direction indicated essential impact on stability limits. Tunc et al.[4] researched the varying dynamics of the hexapod robotic structure by using impact hammer analysis method. It was discovered that the dynamic reaction, both low and high frequencies, at the tool tip may change regarding the robot position. Additionally, it was shown that because of the structural flexibility of the hexapod robotic platform, asymmetrical tool tip dynamics was observed. In such cases, feed rate

direction and robot configuration serve as a remarkable identification of the stable cutting conditions. It can be concluded that these frequencies are in a low frequency band compared to CNC machines and robot milling is significantly more inclined to low-frequency chatter especially at low spindle speeds.

In this paper, it is planned to show that the kinematic redundancy in 6-axis serial arm robots can be utilized to expand stability limits and avoid chatter. From this time forward, the paper is sorted out as pursues; the kinematics of serial arm robots is introduced in Section 2. This is trailed by the dynamics of robot and stability of robotic milling in Section 3. In view of the theoretical foundation given in Section 2 and Section 3, the experimental examination on the impact of kinematic redundant configuration on tool tip dynamics is exhibited in Section 4. The experimental section is finalized with conclusions and discussions subsequent to showing the stability simulations in Section 5.

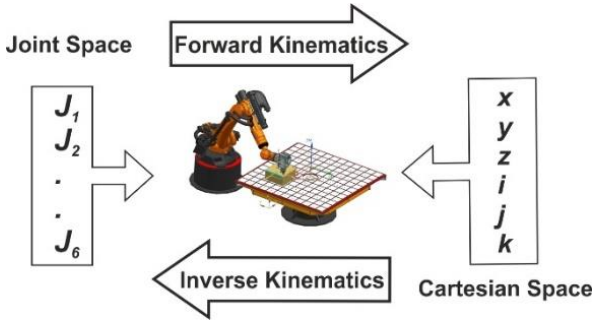

Figure 1: Kinematics of serial arm industrial robots.

2 Kinematic Description of the 6-axis serial arm robot

Robotic mechanisms comprise of links associated with one another by rotational joints. The kinematic analysis is performed in two different ways, forward and inverse to change by transformations from joint directions to workpiece coordinates and the other way around as delineated in Figure 1. KUKA KR240 R2900 6-axis serial arm robot was used to accomplish point of this work as a milling robot. Robot kinematics was settled dependent on the methodology proposed by Denavit and Hartenberg [8] utilizing 4x4 homogenous transformation matrices. In milling applications, the tool posture is defined by the tool tip position and tool axis. The translational movement is defined by 3D position x, y, z and the tool axis orientation are defined by a unit vector i, j, k components as appeared in Figure 1.

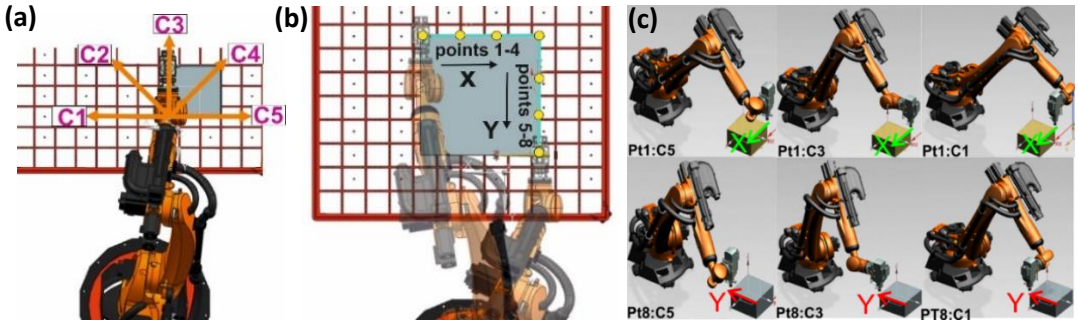

Figure 2: Configuration redundancy in robotic milling a) definition of configurations b.) Representative tool path directions c.) Representative robot configurations on the tool path

3 Dynamics and Stability of Robot and Milling Operation

Dynamic equations can be derived from Lagrange-Euler formulation due to its well-organized structure depends on energy calculations. To derive equations for 3D robot mechanisms, Fu et al.[9] is presented a

model that contains inertial effects of the manipulator by using inertia tensor. Usage of transformation matrices and derivatives of transformations that is defined as a multiplied by a constant coefficient matrix of transformation matrices is useful to evaluate dynamics. First, kinematic equations should be written in a transformation matrix form for 6-axis serial arm robot.

$$T_i = \frac{d}{dt}\left(\frac{\partial L}{\partial \dot{\theta}_i}\right) - \frac{\partial L}{\partial \theta_i}$$

Where L is lagrangian symbol that defines difference between kinetic energy and potential energy depends on joint position, velocity and acceleration (kinetic energy less potential energy). According to model that is presented by Fu et al.[9], it is written as follows.

$$T_i = \sum_{k=1}^{n} D_{ik}\ddot{q}_k + \sum_{k=1}^{n}\sum_{m=1}^{n} h_{ikm}\dot{q}_k\dot{q}_m + C_i$$

In a matrix form;

$$T = D(q)\ddot{q} + h(q,\dot{q}) + C(q)$$

Where $D(q)$ is inertia matrix, $h(q,\dot{q})$ is vector of coriolis and centrifugal forces and $C(q)$ is the vector of gravitational forces. Cartesian stiffness matrix and mass matrix are required to calculate base frequencies without an external force, using the homogeneous solution of the characteristic equation of motion.

$$\det([K] - [D]\lambda^2) = 0$$

Where K and D are stiffness and mass matrix in cartesian space. $D(q)$ and $K(q)$ can be converted to cartesian coordinate formats by multiplying Jacobian.

$$D = (J^{-1})^T D(q) J^{-1}$$

$$K = (J^{-1})^T K(q) J^{-1}$$

Where λ is the angular frequency of which is calculated by using mass matrix and stiffness matrix at various confguration and positions. Natural frequency can be obtained by the following equaiton.

$$f = \frac{\lambda}{2\pi}$$

According to technical specifications of the KUKA KR240 , axes limits are determined and all the joints are moved 130 degrees. In each position and related configuration, natural frequencies and loss factors are calculated.

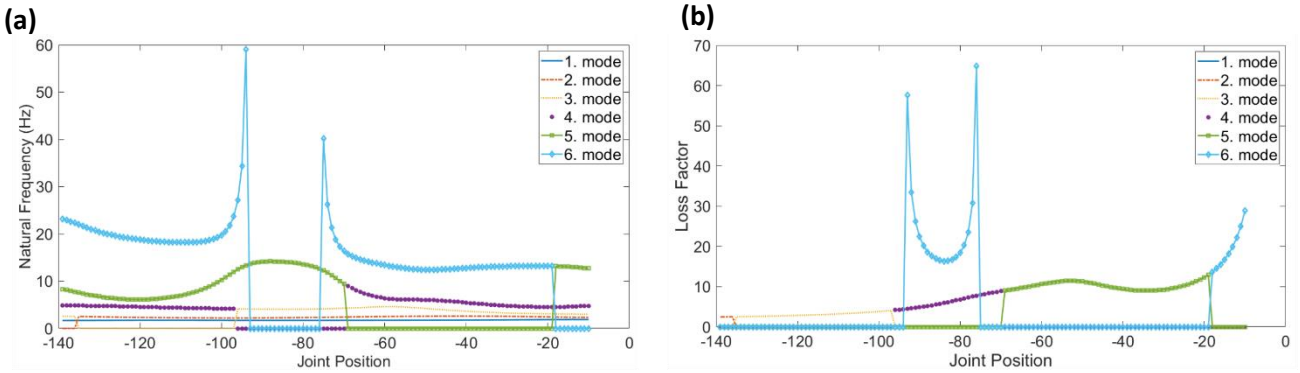

Figure 3: (a) Natural frequencies versus joint positions (b) Loss factors versus joint positions

The tool tip dynamics is coupled response of robot structure, spindle, tool holder and the tool as shown in Figure 4. In such a coupling, the robot dynamics vary throughout the workspace, where the dynamics of the other components are assumed to be not changing. The contribution of the robot dynamics to tool tip frequency response function (FRF) depends on the robot kinematics, which is mathematically represented as the Jacobian matrix. Thus, its contribution to tool tip FRF varies with configuration and position. In this regard, the kinematic redundancy comes into consideration in adjusting the directional contribution of the robot dynamics to tool tip FRF, which is governed by the kinematic redundant rotation of the robot wrist around the tool axis as shown in Figure 2a and Figure 2c.

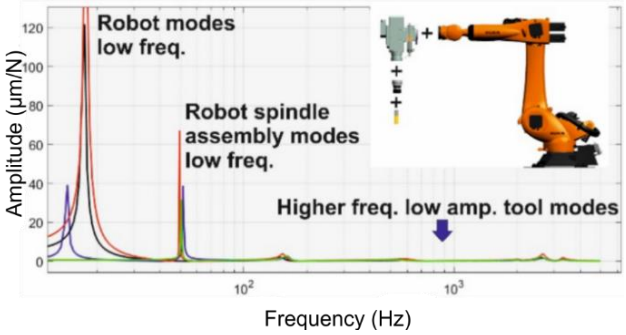

Figure 4: Coupled response in robotic milling.

Taking into account that, the stable cutting depth is related to the FRF in two directions, Gxx and Gyy, as analytically solved in the frequency domain for end milling operations the variation in the tool tip dynamics affects the stability lobes [7].

$$a_{lim} = -\frac{2\pi\Lambda_R}{NK_t}(1+\kappa^2)\text{ere, } \Lambda = -\frac{1}{2a_0}\left(a_1 \pm \sqrt{a_1^2 - 4a_0}\right) \quad (1)$$

4 Experimental investigation on the effects of kinematic redundancy on tool tip FRF

First, the effects of the kinematic redundancy on tool tip FRF are investigated at various robot configurations in such a way that the spindle redundantly rotates around the tool axis as shown in Figure 2a. The impact of robot position on the tool tip FRFs, Gxx and Gyy, is observed by partitioning the robot path into 4 points along X and Y directions as appeared in Figure 2b. At each position, the tool tip FRF is measured through impact hammer tests, at 5 different configurations.

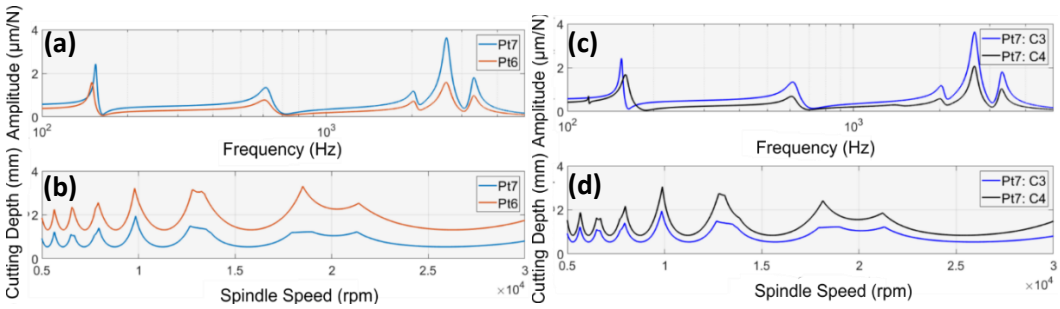

Figure 5: Effect of FRF variation on stability lobes. (a) FRF at Pt6 and Pt7 (same configuration); (b) Position dependency of stability diagrams; (c) FRF at Pt7 at different configurations (same position); (d) configuration dependency of stability diagrams.

FRF measurements are performed on a representative carbide Ø12 flat end mill. To measure the tool tip dynamics at higher frequencies 2301-Endevco-Meggitt mini-modal hammer is used, where the vibration is measured by the uniaxial accelerometer, 352C22 PCB-PIEZOTRONICS. CutPro© simulation software is used for FRF measurements. The variation in natural frequency and FRF amplitudes, affect the location of stability

pockets in terms of spindle speed and stability limits, respectively in Figure 5. In Figure 5a, it is seen that the tool tip FRF varies in terms of amplitude and natural frequency almost at all modes. This reflects the stability diagrams as shown in Figure 5b. A similar observation is valid for the effect of robot configuration on the tool tip FRF in Figure 5c. Reflection of the configuration effect on the stability diagrams is clearly observed in Figure 5d.

4.1. Repeatability analysis

The repeatability of the FRF measurements is investigated to clearly identify the effect of robot configuration on the FRFs. For such a purpose, the FRF measurement at the tool tip is repeated 5 times when the robot is at Pt 8 and configuration C1. Then, the variation among the repeated measurements is compared with the measurements done at different robot configurations as shown in Figure 6.

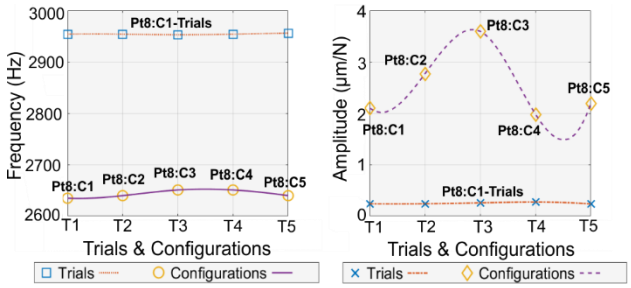

Figure 6: Comparison on Trial and Configuration Variations

In Figure 6, it can be observed that the natural frequency of the 2nd tool mode is repeatably measured, which confirms that the measurement repeatability is reasonably good. The 2nd natural frequency of the tool mode varies from 2953 Hz to 2956 Hz among the repeated tests, whereas it varies from 2635 Hz to 2651 Hz among configuration C1 to C5. As the variation of the 1st mode amplitude is concerned, the amplitude does not change significantly among the repeated tests, however the amplitude shows a variation in the range of 1.98 µm/N to 3.60 µm/N, i.e. 80%. Therefore, it can be concluded that measurement errors do not have remarkable impact on stability lobes.

4.2. Effect of robot position

The measured FRFs at eight different positions of the robot, at the same configuration, are plotted in Figure 7, where the modes contributed by the robot, spindle, tool holder and tool are seen.

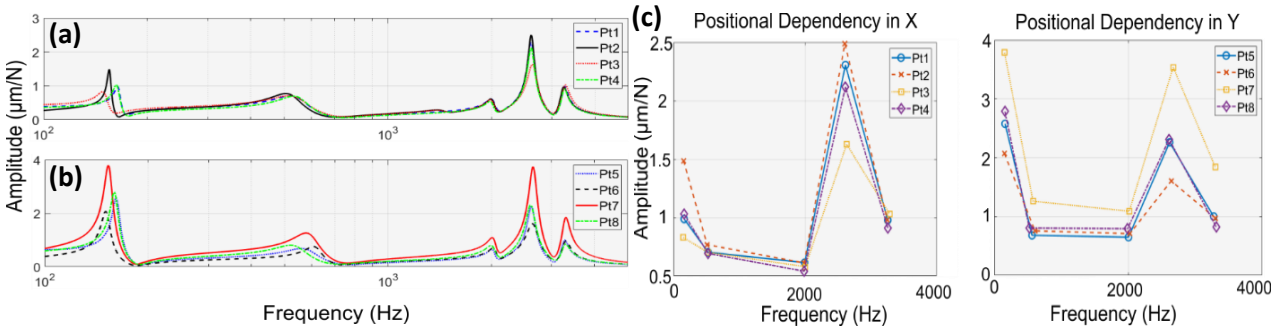

Figure 7: Change in tool tip FRF as robot moves in (a) X direction; (b) Y direction; (c) Positional dependency in both directions

In total, 5 modes are observed in the FRF plot. Two of which are at the lower frequency region, which are 150 Hz and 550 Hz, respectively. Three significant modes are observed contributed by the tool, which are around 2300 Hz, 2600 Hz and 3100 Hz, respectively. The variation of each mode in terms of natural frequency and amplitude are shown in Figure 7a and Figure 7b. In Figure 7c, position dependency is evaluated regarding

same configuration. C2 and C3 configurations are used for X and Y directions, respectively. These configurations are used for all the FRF measurement points on the tool-path (see Figure 2b) in both directions due to a clear observation of most deviated FRFs. In X direction, maximum deviation is observed near 2630 Hz between Pt2 and Pt3. Most flexible tool mode reached to 2.489 µm/N at Pt2 and most rigid tool mode is determined as 1.627 µm/N at Pt3. Flexibility is increased by 53%. In low-frequency band that around 160 Hz, FRFs indicate similar results at different amplitudes in terms of positional effect. In Y direction, most rigid and most flexible modes at the tool tip are observed at Pt6 and Pt7, respectively. Dynamic compliance of the most flexible tool is reached to the 3.5 µm/N and most rigid tool mode appeared as 1.6 µm/N. Flexibility increased tremendously as compared to most rigid tool mode and increased flexibility is higher than two times of the most rigid tool mode. In the next section, flexibility and rigidity variations are investigated and discussed in detail regarding to positions and mostly configurations.

4.3. Effect of robot configuration

The measured FRFs at 5 different configurations of the robot, at the same position, are plotted in Figure 8, where the modes contributed by the robot, spindle, tool holder and tool are seen.

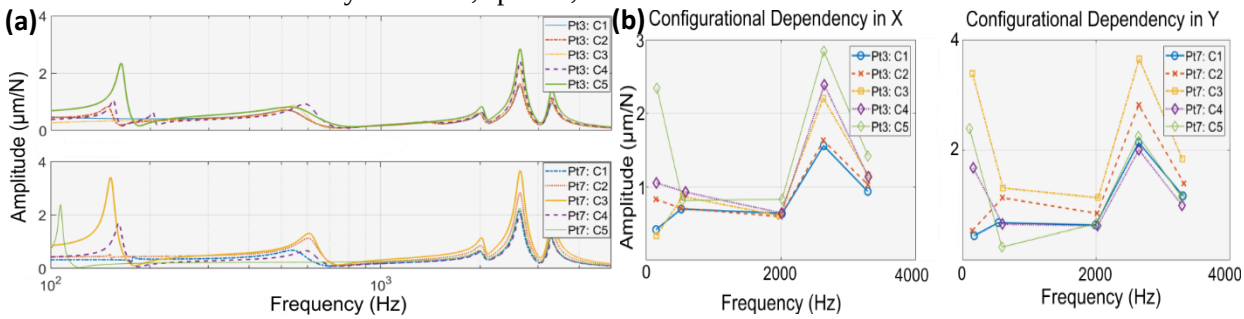

Figure 8: (a) Variation of natural frequency and amplitude of the significant modes at varying robot configurations at the Pt3 and Pt7; (b) Configurational dependency in both directions

5 modes are observed in the FRF plot. Two of which are at the lower frequency region, which are 160 Hz and 570 Hz, respectively. Three significant modes are observed contributed by the tool, which are around 2000 Hz, 2600 Hz and 3300 Hz, respectively. The variation of each mode in terms of natural frequency and amplitude are shown in Figure 8a. In Figure 8b, configurational dependency is evaluated regarding same positions in X and Y directions. FRFs are measured for all configurations at Pt3 and Pt7, respectively. Pt3 and Pt7 are selected due to significant changes in FRF measurements with respect to configuration variations. Maximum deviation is observed around 2640 Hz at Pt3 and Pt7 with respect to all configurations. Most flexible tool mode reached to 2.8 µm/N at C5 in Pt3 and most rigid tool mode is determined as 1.6 µm/N at C1 in Pt3. Flexibility is increased around 83%. Most flexible tool mode reached to 3.7 µm/N at C3 in Pt7 and most rigid tool mode is determined as 2.0 µm/N at C4 in Pt7. Flexibility is increased around 82% as compared to the most rigid tool mode. At low frequency band around 100 Hz, FRFs are observed and the trend of the changes is similar with different amplitudes in terms of configurational factor. Investigation of the FRFs at varying configurations and progressive points along a representative tool path provides the intuition about selection of the robot configuration for increase stability. However, for selection of the robot configuration along the tool path stability analysis is required as discussed in the next section.

5 Stability analysis

To investigate the effects of robot configuration and identify the configurations sustaining increased stability along the tool path, stability analysis is performed by using the obtained tool tip FRFs and workpiece material regarding to process parameters. Workpiece material is selected as Aluminum 6061-T6 due to broad range of applications in industry. Carbide flat end mill with 12 mm diameter is used for the milling operation. Radial

depth of cut is determined as 6 mm (half immersion). Milling type is determined as down milling and feed per tooth is selected as 0.2 mm/rev/tooth. The effect of robot configuration on stability diagrams is plotted in Figure 9a, for the representative position (Pt7), when the feed direction is along Y axis.

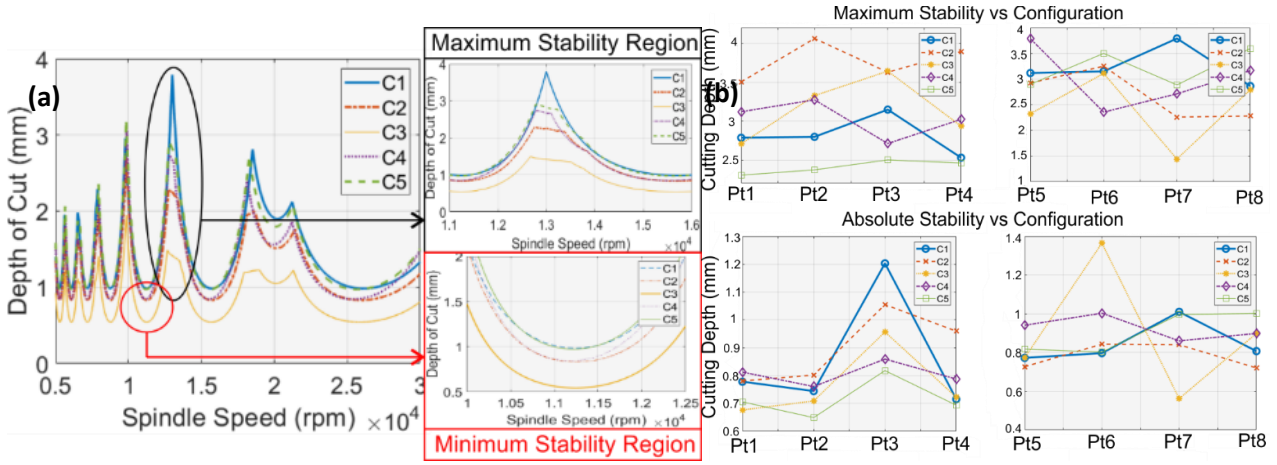

Figure 9: (a)Stability lobe plot for maximum deviated stability limits w.r.t. configurations (b) stability limits versus configurations

According to the stability diagrams, preferable robot configurations can be identified at progressive positions along the tool path for increased stability. The comparisons are performed in terms of both absolute stability limit and the maximum stability limit in the common stability pockets. Figure 9a shows that at Pt7 configuration C1 provides increased stability with the maximum stable cutting depth of 3.79 mm at 12850 rpm, where the absolute stability is 1 mm. Through a similar comparison, the preferable configurations are identified at the other points along the tool path as plotted in Figure 9b. When the feed direction is along the X axis, in case absolute stability limit is used as the criterion the preferable robot configurations are C4, C2, C1 and C2. In terms of the maximum stability limits at the stability pockets, the preferable configurations are C2, C2, C2, C2. When the feed rate direction is along the Y axis, in case absolute stability limit is used as the criterion the preferable robot configurations are C4, C3, C1 and C4. In terms of the maximum stability limits at the stability pockets, the preferable configurations are C4, C5, C1, C5. In this regard, it was shown that the preferable robot configuration may change along the tool path in terms of absolute stability and maximum stability.

6 Results & Discussion

In this study, as well as the impact of positional dependency on tool tip dynamics, effects of the robot configuration on the tool tip dynamics and milling stability are analyzed through FRF measurements and stability simulations. Maximum stability limits and absolute stability limits are utilized as a correlation paradigm for determination of the robot configuration all through the tool path. For the situation that configuration adjustments are chosen dependent on absolute stability, reasonable deviations are observed among configurations. In this way, preferable configurations along large region tool paths may should be chosen dependent on the absolute stability limits. Rather than changing workpiece place and generated tool-path, configuration can be changed on the same workspace and milling operation continues processing within the range of predetermined stability limits. Positional dependency of stability limits in robotic milling is well-known, which can be compensated by changing the robot configuration as demonstrated in this study. Even at the same position, robot can be dodged from the chatter vibration by using different configuration as it influences the tool tip dynamics.

Acknowledgement

The authors acknowledge the support of TUBITAK under grant number 217M078 and 217M210.

7 REFERENCES

[1] Quintana G, Ciurana J. Chatter in machining processes: A review. International Journal of Machine Tools and Manuf. 2011; 51(5):363-76.

[2] Oki Y, Kanitani K. Development of robot machining system for aluminum building materials. J JSME. 1996; 99(937):78-87.

[3] Pan Z, Zhang H, Zhu Z, Wang J. Chatter analysis of robotic machining process. Journal of materials processing technology 2006; 173(3):301-9.

[4] Tunc LT, Shaw J. Experimental study on investigation of dynamics of hexapod robot for mobile machining. The International Journal of Advanced Manufacturing Technology 2016; 84(5-8):817-30.

[5] Mejri S, Gagnol V, Le TP, Sabourin L, Ray P, Paultre P. Dynamic characterization of machining robot and stability analysis. The International Journal of Advanced Manuf. Tech. 2016; 82(1-4):351-9.

[6] Bisu C, Cherif M, Gérard A, K'nevez JY. Dynamic behavior analysis for a six axis industrial machining robot. In Advanced Materials Research 2012 (Vol. 423, p. 65-76). Trans Tech Publications.

[7] Altintaş Y, Budak E. Analytical prediction of stability lobes in milling. CIRP annals. 1995; 44(1):357-62.

[8] Denavit J. A kinematic notation for low pair mechanisms based on matrices. ASME J. Appl. Mech. 1955; 22:215-21.

[9] Fu, King Sun, Ralph Gonzalez, and CS George Lee. *Robotics: Control Sensing. Vis*. Tata McGraw-Hill Education, 1987.